

Automated detection of myocardial infarction from ECG signal using variational mode decomposition based analysis

Ato Kapfo , Samarendra Dandapat, Prabin Kumar Bora

Department of Electronics and Electrical Engineering, Indian Institute of Technology, Guwahati, Assam 781039, India

✉ E-mail: ato.kapfo@iitg.ac.in

Published in Healthcare Technology Letters; Received on 22nd February 2020; Revised on 21st September 2020; Accepted on 6th November 2020

In this Letter, the authors propose a variational mode decomposition method for quantifying diagnostic information of myocardial infarction (MI) from the electrocardiogram (ECG) signal. The multiscale mode energy and principal component (PC) of multiscale covariance matrices are used as features. The mode energies determine the strength of the mode, and the PCs provide the representation of the ECG signal with less redundancy. K-nearest neighbour and support vector machine classifier are utilised to assess the performance of the extracted features for the detection and classification of MI and normal (healthy control). The proposed method achieved a specificity of 99.88%, sensitivity of 99.90%, and accuracy of 99.88%. Experimental results demonstrate that the proposed method with the multiscale mode energy and PC features achieved better output compared to the previously published work.

1. Introduction: Myocardial infarction (MI) is the major cause of death among cardiovascular diseases according to the report from the World Health Organisation (WHO) [1]. The electrocardiogram (ECG) is used widely to diagnose heart-related diseases, including MI because it is efficient, effective, and non-invasive. Multichannel ECG records the three-dimensional view of the human heart, and it captures the pathological characteristics and morphological changes of MI.

The pathogenesis of MI begins as a result of the plaques, a substance mostly made of fat, fibrin, and platelets get deposited in the inner surface of the coronary arteries causing disruption and occlusion of the circulation of blood to a portion of the heart [2]. The myocardium is starved of oxygenated blood, and abundant nutrients and a condition occurs called cardiac ischemia. When the ischemia lasts for an extended period, the heart tissue dies, leading to MI, commonly known as a heart attack. During MI, the morphology of the multi-lead ECG signal will vary from their normal characteristics. The anomalies of MI in ECG waveform evolve through the following sequence [2]:

- (i) *ST-segment elevation*: This change depends on the gender and age of MI patients.
- (ii) *Hyperacute T waves*: This wave is tall, pointed, and symmetric in at least two consecutive leads [3]. T wave inversion appears after hyperacute T wave.
- (iii) *Q waves abnormality*: The Q wave is considered pathological if its duration is >0.04 s in the leads I, II, III, and aVF, or leads V3–V6.

The normal ECG and the evolution of two pathological characteristics of MI are shown in Fig. 1. The normal ECG for reference concerning pathological cases is shown in Fig. 1a. The change of morphology of ECG due to MI is depicted in Figs. 1b and c. Over the past several decades, automated detection and classification of MI have been studied and developed based on the amalgamation of feature extraction using signal processing tools and machine learning algorithms. In feature extraction stage, several studies were adopted to capture the pathological characteristics which indicate the signature of MI such as Q-wave, ST-segment deviation, T-wave integral, T-wave amplitude and integral of single ECG cycle [4–7]. The pyramidal multiresolution decomposition

technique of discrete wavelet transform (DWT) using different mother wavelets such as db4, db6 is a popular method for identification of MI [8, 9], and some works have implemented Daubechies biorthogonal wavelet [10, 11]. Empirical mode decomposition (EMD) was used for feature extraction to discriminate between normal and MI [8]. In [12] principal component analysis (PCA) is implemented for different orders of polynomial approximations and concluded that the 12 principal components (PCs) were found to be effective for the detection of MI. Alternatively, Liu *et al.* [13] use polynomial function and treated polynomial coefficients as features to classify MI patients and healthy controls. In the classification stage, the extracted feature vectors are fed as input to different classification algorithm for detecting MI. The most popular algorithms for classification are support vector machine (SVM) [11, 12, 14], K-nearest neighbour (KNN) [8, 15], neural network [16, 17], decision trees [13, 18], and random forests [19].

In this work, the authors' objective is to establish a new method for automated detection of acute MI. Variational mode decomposition (VMD)-based feature extraction is proposed in this study. The main advantage of the VMD technique over the other decomposition techniques, such as empirical mode decomposition (EMD) is that it is built on a sound foundation of mathematical theory. In contrast, the latter lacks and is sensitive to noise and sampling. One caveat of DWT for analysis of MI is the hard band-limits of wavelet and inability to select appropriate mother wavelets. The VMD method has the edge over wavelet transform multiresolution technique because the latter one requires a predefined basis function like Daubechies, Symlet, Daubechies biorthogonal, etc. Implementation of different wavelet functions can result in a different outcome. Hence, the DWT efficiency depends on the choice of the mother wavelet and the decomposition level. In the existing literature, there is no proper justification for the use of a particular mother wavelet. So the selection of mother wavelet and analysis based on wavelet transform is a challenging task. In contrast, VMD is a data-driven and adaptive, decomposition model that assesses the relevant bands, and determines the associated modes simultaneously. This decomposition algorithm can reconstruct the decomposed ECG signal optimally (perfectly or in a least-squares sense). The main building blocks of VMD are the Wiener filter for denoising, the Hilbert transform to obtain single-side (non-negative) spectrum, and the harmonic mixing to

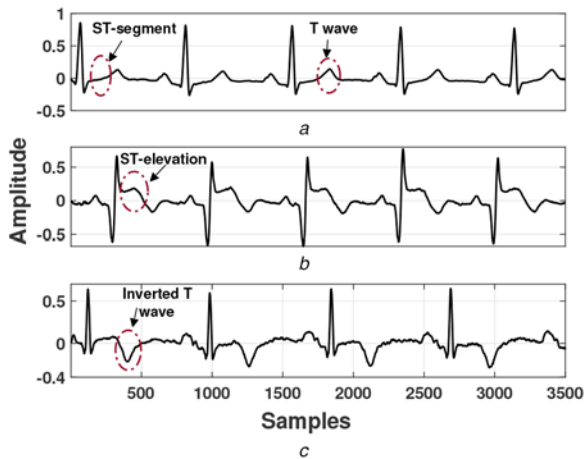


Fig. 1 Normal ECG and the evolution of MI
a Normal ECG signal
b, c Pathological characteristics observed due to MI

translate the frequency spectrum to the baseband. Due to these inherent properties ingrained in this decomposition model, it outperforms its decomposition counterparts vis-à-vis EMD and DWT. The VMD method is a recently introduced decomposition technique that decomposes the AM-FM signal into multiple subbands. It has gained wide popularity since its inception to analyse one-dimensional signals, such as in grid-connected distributed generation system, epileptic seizure detection from the EEG signals, and estimation of electroglottographic (EGG) signals [20–22]. The VMD technique is found to be effective to eliminate noise, baseline wandering, and detection of cardiovascular diseases of the ECG signal. Prabhakararao and Manikandan [23] have used the VMD method to extract baseline wander using frequency criterion and then subtract from the original signal. The performance results of their study ascertained that the VMD algorithm can effectively get rid of the baseline wanders without mangling the vital clinical information of the ECG signal. Lahmiri *et al.* [24] have used VMD and DWT for denoising of ECG signals. Tripathy *et al.* [25] decompose the ECG signal into five modes and extracted three different features from the first three modes for the detection of an arrhythmia. To the best of our knowledge, there is no article in the literature reporting MI diagnosis using VMD technique. Therefore, in this paper, we propose a new algorithm for automated detection and classification of acute MI from HC subjects using 12-lead ECG signals.

The remaining portions of this Letter are structured as follows. The proposed VMD-based method to extract features that are related to MI, including preprocessing of an input ECG signal is described in Section 2. Furthermore, in Section 3, the ECG database used in this work is introduced briefly and presents the results and discussions in detail. In Section 4 conclusions are drawn.

2. Method: The structure of the proposed method contains four main stages: preprocessing and beats segmentation, decomposition of the MEGC signal by VMD method, feature analysis, and binary classification of the extracted features between MI and HC, as shown in Fig. 2.

2.1. Preprocessing: MEGC signal is corrupted with various types of noise. The preprocessing involves filtering unwanted noise and artefacts from a raw ECG signal. A moving average filter is utilised to remove the low-frequency baseline wandering [26]. The frame-based processing of MEGC exploited the inter-lead, intra-beat, and intra-sample correlation information of the MEGC signal [27]. This information can facilitate to diagnose various CVD, including MI. The beat segmentation of the noise-free

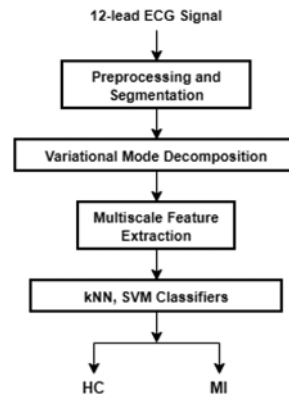


Fig. 2 Block diagram for detection of MI from multi-lead ECG

MEGC signal is carried out by detecting R-peaks using Pan Tompkins algorithm, and segment 250 samples and 400 samples to the left of R-peaks and to the right of R-peaks, respectively, resulting in 651 points in each sample at a sampling rate of 1 kHz [28, 29]. The first and last beats in all the datasets were excluded to maintain uniformity of the segmented beats. The R-peaks of lead I are used as a reference point to segment the remaining leads of MEGC signals since all the 12 leads are recorded simultaneously. Each ECG beat has 651 samples, which covers all the characteristics of the ECG cycle.

2.2. Proposed method: VMD method adaptively decomposes MEGC signal into a K ensemble number of band-limited sub-signals or principal modes v_k , where the modes are compactly supported around their centre frequency [30]. The H^1 Gaussian smoothness determined the bandwidth of each mode of the shifted signal. The resulting constrained problem is formulated as

$$\min_{\{v_k\}, \{\omega_k\}} \left\{ \sum_{k=1}^K \left\| \partial_t \left[\left(\delta(t) + \frac{j}{\pi t} \right) * v_k(t) \right] e^{-j\omega_k t} \right\|_2^2 \right\} \quad (1)$$

$$\text{s.t.} \quad \sum_{k=1}^K v_k(t) = v(t)$$

where $v(t)$ is the ECG signal, $\{v_k\} := \{v_1, v_2, \dots, v_K\}$ represents the set of decompose modes, $\{\omega_k\} := \{\omega_1, \omega_2, \dots, \omega_K\}$ denotes the set of each centre pulsation corresponding to the k th mode, t is the time the number of modes is signified by K , ∂_t stands for the differential operation, and $*$ is the convolution.

The constrained problem of (1) can be addressed by introducing Lagrangian multiplier and quadratic penalty term are employed to make the problem unconstrained. The augmented Lagrangian function is expressed as follows:

$$\mathcal{L}(\{v_k\}, \{\omega_k\}, \lambda) = \alpha \sum_k \left\| \partial_t \left[\left(\delta(t) + \frac{j}{\pi t} \right) * v_k(t) \right] e^{-j\omega_k t} \right\|_2^2$$

$$+ \left\| f(t) - \sum_k v_k(t) \right\|_2^2 + \langle \lambda(t), f(t) - \sum_k v_k(t) \rangle \quad (2)$$

where $\lambda(t)$ denotes the Lagrangian multiplier, α is the balancing parameter that control bandwidth, and $\delta(\cdot)$ is the Dirac distribution. An optimisation technique called alternate direction method of multipliers (ADMM) is rendered to solved (2). All the modes

gained is obtained in the Fourier domain and is given as

$$\hat{v}_k^{n+1}(\omega) = \frac{\hat{f}(\omega) - \sum_{i \neq k} \hat{v}_i(\omega) + (\hat{\lambda}(\omega)/2)}{1 + 2\alpha(\omega - \omega_k)^2} \quad (3)$$

The optimisation of w_k also takes place in the Fourier domain, the updated equation of w_k is shown as

$$\omega_k^{n+1} = \frac{\int_0^\infty \omega |\hat{v}_k(\omega)|^2 d\omega}{\int_0^\infty |\hat{v}_k(\omega)|^2 d\omega} \quad (4)$$

VMD is a parameterised method, and it has to initialise two tuning parameters in advance. These parameters are the bandwidth control parameter (α), and the number of modes (K) to be decomposed from the ECG signal. The correct choice of the values of α , and K capture the characteristics of the ECG signal in different decomposition mode. The experimental results reveal that a big value of α permits a low bandwidth in the decomposed modes. This results in mode mixing and also causes spurious mode in the higher level of mode decomposition. On the other hand, small values of α give rise to noise in the estimated mode. In this analysis, we have found that the corresponding parameters α of 1400 and K of 5 are considered the optimised parameters as it can capture the relevant components of the ECG signal. The different modes of the healthy control signal by VMD are illustrated in Figs. 3–5. Figs. 3a, c, 4a, c, 5a show the time-domain signals of the first mode, second mode, third mode, fourth mode, and fifth mode, respectively, and Figs. 3b, d, 4b, d, 5b depict the corresponding frequency spectra of the decomposed

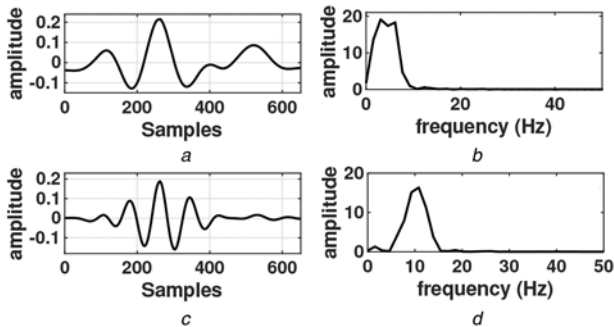


Fig. 3 Visualization of VMD mode 1 and mode 2 and its corresponding spectrum

- a Decomposed HC signal of mode 1
- b Mode 1 spectrum
- c Decomposed HC signal of mode 2
- d Mode 2 spectrum

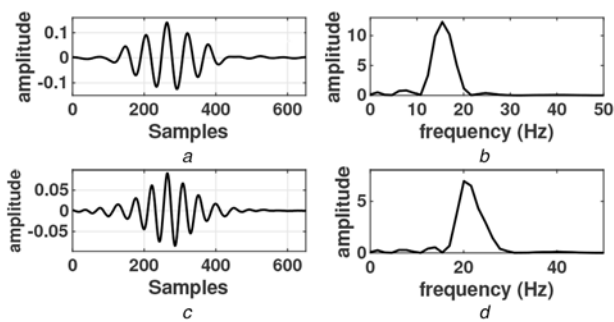


Fig. 4 Visualization of VMD mode 3 and mode 4 and its corresponding spectrum

- a Decomposed HC signal of mode 3
- b Mode 3 spectrum
- c Decomposed signal of mode 4
- d Mode 4 spectrum

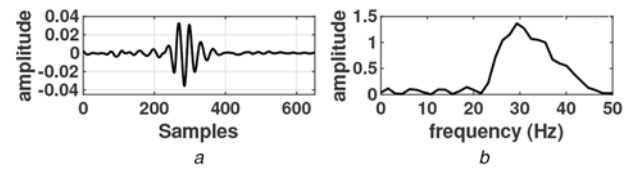


Fig. 5 Visualization of VMD mode 5 and its corresponding spectrum
a Decomposed HC signal of mode 5
b Mode 5 spectrum

mode. The dominant frequency of the spectrum of mode 1 is 3 Hz, which captures the P-wave and the T-wave. Mode 2 and mode 3 contain the characteristics of the QRS complex, and its dominant frequencies are around 12 and 15 Hz, respectively. The spectrum of mode 4 and mode 5 depicts that the higher frequency of the QRS complex is observed in these two modes. Their dominant frequencies are 20 and 28.4 Hz, respectively.

When the standard 12 leads ECG is decomposed with the same number of mode, it results with an equal number of k th mode coefficient at the j th level. Mode coefficients obtained from the decomposition are arranged in the matrices. The rows correspond to mode coefficients while the columns represent the corresponding ECG leads. The mode matrix is given by

$$M_j = [cM_{j,k}^1, cM_{j,k}^2, \dots, cM_{j,k}^i] \quad (5)$$

where k is coefficients and $i = 1, 2, \dots, 12$ is the number of leads.

Assuming that the significant information of the ECG signal will reflect in the distribution of energy in different decomposition levels, the energy can be computed at different modes. The energy obtained from the coefficients along each decomposed mode is considered as multiscale mode energy [9, 11], and it is given as

$$E_{cM_{j,k}^i} = \frac{\sum_{k=1}^{N_j} [cM_{j,k}^i]^2}{N_j} \quad (6)$$

where N_j is the number of coefficients. In this study, the multiscale mode energy features from five decomposed modes of 12-standard leads are evaluated. Five multiscale mode energies of 12 features are extracted from one mode matrices. A total of 60 multiscale mode energies are chosen from the five mode matrices.

MI causes variation in electrical conduction properties of heart tissues due to obstruction in the inside wall of the coronary artery. These variations in values lead to a change in the morphological features of ECG signals, and they can be captured in different modes when subjected to the VMD algorithm, as shown in Figs. 3–5. In order to quantify these changes, covariance structures of the multiscale mode matrices (MSMMs) are analysed. When eigenanalysis is computed on mode matrices, the clinical diagnostic information related to MI presumably appears in eigenspaces. The covariance matrices are assessed from the MSMM, and it is evaluated as [31]

$$C_{M_j} = \frac{1}{(N_j - 1)} \left([M_j]^T [M_j] \right) \quad (7)$$

where C_{M_j} is the covariance matrix at the j th mode. When (7) is subjected to eigendecomposition the expression appears in the following equation:

$$C_{M_j} V_{M_j} = V_{M_j} \Lambda_{M_j} \quad (8)$$

where Λ_{M_j} and V_{M_j} are the eigenvalues and eigenvectors of the mode matrix, respectively. Eigenvector matrix V_{M_j} diagonalise

the covariance matrix C_{M_j} as

$$V_{M_j} C_{M_j} V_{M_j}^{-1} = \Lambda_{M_j} \quad (9)$$

Λ_{M_j} is the diagonal matrix. The eigenvalues are the diagonal elements of the diagonal matrix. The eigenvectors constitute the vector directions of the new feature space of the covariance matrix, and the eigenvalues represent the magnitudes of those vectors. The eigenvector corresponding to the highest eigenvalue is the first PC. The eigenvalues are sorted from largest to smallest value and accordingly, the corresponding eigenvectors as it provides the significance of the components. The ordered eigenvalues in the mode matrix are

$$\lambda_{M_{j_1}}, \lambda_{M_{j_2}}, \lambda_{M_{j_3}}, \dots, \lambda_{M_{j_N}} \quad (10)$$

In this work, six dominant eigenvalues from a single covariance matrix are evaluated to create feature vectors. A total of 30 feature vectors are extracted from five covariance matrices.

2.3. Classifiers and performance measures: Two supervised learning classifiers, KNN, and SVM are used to carry out the classification task of HC and MI. KNN is a non-parametric algorithm employed for classification and regression problems. The algorithm predicts the target label by discovering the KNN of the test data by using distance measures. In this analysis, we have used Euclidean distance and $K=5$.

SVM is a two-category classification model defined by a separating hyperplane. The algorithm outputs the given labelled training data by defining optimal hyperplane in an N -dimensional space which categorises the test feature set [32]. The training features set is (x_m, y_m) , $m = 1, 2, \dots, n$, $x \in \mathbf{R}^l$, $y \in (+1, -1)$. The feature matrix of input multi-lead ECG can be represented, $\mathbf{Z} \in \mathbf{R}^{j \times k}$ with each feature vector $z_m \in \mathbf{R}^k$, $i \in 1, 2, \dots, j$, where j is the number of feature sets, and k is the length of the feature vector and ($k=90$). The optimisation is based on the maximisation of the hyperplane, given by

$$\min \frac{1}{2} \mathbf{w}^T \mathbf{w} + C \sum_{m=1}^j \varepsilon_m \quad (11)$$

subjected to $y_m(\mathbf{w}^T \phi(x_m) + b) \geq 1 - \varepsilon_m$, $\varepsilon_m \geq 1$, where w is the hyperplane, and C is the regularisation parameter. The kernel function $\phi(x_m)$ transform the training feature set (x_m) to the high-dimensional space. The constrained problem of (11) is translated into the Lagrangian dual problem in order to make the problem unconstrained. The dual quadratic optimisation problem produce a new equation, given by

$$\max_{\mu} L(\mu) = \sum_{m=1}^q \mu_m - \frac{1}{2} \sum_{m=1}^q \sum_{n=1}^q \mu_m \mu_n y_m y_n R(z_m, z_n) \quad (12)$$

subjected to $0 \leq \mu_m \leq C$, $m = 1, 2, \dots, n$ and $\sum_{m=1}^q \mu_m y_m = 0$. μ_m is the Lagrange multiplier for every training point. The predicted output y_p for the test feature subset z_t from MCEG is computed as

$$y_p = \text{sgn} \left[\sum_{m=1}^{\hat{q}} \mu_m y_m R(z_m, z_t) \right] \quad (13)$$

where $R(z_m, z_t)$ is the kernel function and \hat{q} is the support vector. In this study, the linear kernel and radial basis function (RBF) kernel

are used. The RBF kernel used in this work is given as

$$R(z_m, z_t) = \exp\left(\frac{\|z_t - z_m\|^2}{2\sigma^2}\right) \quad (14)$$

where the variance parameter σ^2 controls the width of Gaussian.

The classifier's performance is assessed using specificity, sensitivity, and accuracy. Specificity (Sp) of a test is the percentage of data that did not have MI and were correctly identified by the test. It is also called the true negative rate. The sensitivity (Se) is defined as the percentage of data that truly had MI and were correctly identified by the classifier. Accuracy (Acc) measurement system is the degree to which the result of a measurement conforms to the correct value. Specificity, sensitivity, and accuracy are then formulated in the following equations:

$$\text{Sp} = \frac{\text{TN}}{\text{FP} + \text{TN}} \times 100 \quad (15)$$

$$\text{Se} = \frac{\text{TP}}{\text{TP} + \text{FN}} \times 100 \quad (16)$$

$$\text{Acc} = \frac{\text{TP} + \text{TN}}{\text{TP} + \text{FP} + \text{FN} + \text{TN}} \times 100 \quad (17)$$

where TP, FP, TN and FN represent the MI patient correctly predicted as MI, healthy patient incorrectly diagnosed as MI, healthy patient predicted as healthy, and MI patient predicted as healthy, respectively.

3. Results and discussion: The ECG data used in this study are taken from the Physikalisch-Technische Bundesanstalt (PTB) database [33]. The 15 concurrently measured signals (standard 12-lead+3 Frank leads) comprise 549 records from 290 subjects. 52 subjects are related to HC, and 148 subjects are related to MI out of 290 subjects. The dataset consists of 81 women, average age 61.6, and 209 men, average age 55.5. The 16-bit resolution over a ± 16.384 mV range of each ECG signal was sampled at 1000 Hz.

The features extracted from the multiscale mode energy and covariance matrices are concatenated and form a 90-dimensional feature vector. These feature subsets are provided as input to the KNN and the SVM algorithm to discriminate the two classes, i.e. healthy control and MI. Each of these feature vectors corresponds to an instance. In this work, 8000, 12,000, and 20,000 instances are utilised for evaluation to investigate the performance of the models. Balanced datasets with a 1:1 class ratio of the instances are implemented for training and testing the classification models since the performance of the classifiers relies on the balance of the dataset to a great extent. In this study, five-fold and ten-fold cross-validation statistical methods are used to ensure the reliability of the predictive models of SVM and KNN classifiers, respectively. The performance of the classification models is shown in Table 1.

With 8000 instances the best performance is obtained for both KNN and SVM linear kernels with the specificity of 86.20 and 96.80%, the sensitivity of 79.20 and 98%, and the accuracy values of 82.70 and 97.40%, respectively. Average specificity, average sensitivity, and average accuracy of SVM with RBF kernel function classifier are found to be 98.88, 99.90, and 99.88%, respectively, for 8000 instances. In this study, the best results for SVM with RBF kernel of $\sigma = 0.5$ are achieved for all the three different instances. The result shows that the less number of instances achieved better results compared to the higher number of instances. This may be because the sample values of the recorded data are different for different subjects. As a result, the variability of the subjects may affect the performance of the classifiers.

Table 1 Performance evaluation for KNN and SVM classifiers

No. of instances	KNN			SVM Lin			SVM RBF		
	Sp, %	Se, %	Acc, %	Sp, %	Se, %	Acc, %	Sp, %	Se, %	Acc, %
8000	86.20	79.20	82.70	96.80	98	97.40	99.88	99.90	99.88
12,000	82.60	77.20	79.20	96.93	97.52	97.22	99.77	99.70	99.73
20,000	77.34	93.20	85.27	96.20	95.93	96.06	99.83	99.89	99.86

Table 2 Summary of the classification performance of the proposed method in comparison with the other existing methods

Author	Number of leads	Database	Techniques and features	Classifier	Performance, %
Sun <i>et al.</i> [19]	12 leads	beat specific HC: 79 records MI: 369 records	ST segment detection multiple instance learning	SVM	Sp=88.1 Se=92.3
Safdarian <i>et al.</i> [6]	1 lead (lead II)	beat specific subjects: 290 subjects	integral of ECG cycle	Naive Bayes	Acc=94.74
Sharma <i>et al.</i> [11]	12 leads	frame specific 1074 frames for MI and HC	DWT multiscale energy multiscale eigenanalysis	SVM	Sp=99 Se=93 Acc=96
Acharya <i>et al.</i> [29]	1 lead (lead II)	beat specific HC: 10,546 MI: 40,182	no feature extraction or feature selection	CNN	Sp=94.19 Se=95.49 Acc=95.22
Liu <i>et al.</i> [35]	4 leads	beat specific HC: 80 records MI: 167 records	no feature extraction or feature selection	multi-lead CNN	Sp=97.37 Se=95.40 Acc=96.22
proposed work	12 leads	beat specific HC: 8000 MI: 8000	VMD multiscale mode energy eigenvalues	SVM	Sp=99.83 Se=99.89 Acc=99.86

From the acquired results of the classification algorithms, the end result of the RBF kernel function of SVM surpassed the SVM with linear kernel function and KNN classifiers. The linearly non-separable input features of the RBF kernel function of SVM is mapped to a high-dimensional feature space [34]. Presumably, this is the reason the RBF kernel function of SVM achieved a better result than KNN and linear kernel SVM.

Summary of the classification results of the proposed method is compared with the previously published works for automated detection and diagnosis of MI and is reported in Table 2. Safdarian *et al.* [6] extracted two time-domain features (integral of T wave and the whole integral of an ECG cycle) to detect MI primarily in the left portion of the heart. The extracted features are given as input to four different classification models, namely, naive Bayes, KNN, multilayer perceptron, and probabilistic neural network. Naive Bayes give the best performance with an accuracy of 94.74%. A new technique to automatically detect MI called latent topic multiple instances learning without labelling heartbeats is developed in [19]. Their study shows specificity values of 88.1 ± 2.3 and sensitivity values of 92.3 ± 0.84 . In [11], DWT decomposed segmented ECG beats up to 6th level of decomposition of standard 12 leads ECG. Multiscale energy features and eigenvalues features are extracted from wavelet subbands to form a 72-dimensional feature vector. Their method for detection of MI obtained specificity, sensitivity, and accuracy of 99, 93, and 96%, respectively. The approach presented in [29] utilised convolution neural network (CNN) algorithm to detect and discriminate the healthy control, and MI ECG beats from single-lead ECG. They analysed the ECG beats with noise-contaminated and noise eliminated and gained 93.53 and 95.22% accuracy, respectively.

Pathological characteristics of MI, such as T-wave inversion, abnormal Q wave, and ST-segment elevation, are regarded by physicians as symptoms of MI [4]. These features are highly dependent on correct delineation and segmentation of the ECG

wave. Hence, the robustness of the extraction of these time-domain features is an issue that must be handled. Several methods using single-lead ECG have been proposed and developed to detect the presence of MI [6, 29]. Liu *et al.* [35] used four leads (aVL, V2, V3, and V5) to detect anterior MI, including anteroseptal MI and anterolateral MI. The segmented ECG beats are used as input to multi-lead-CNN and obtained specificity of 97.37%, sensitivity of 95.40%, and accuracy of 96.00%. Since MI occurs in different leads of MEKG, analysis on all 12 leads will provide more useful information and yield a better result than single lead and fewer leads in detection. In this work, we have used standard 12 leads ECG signal for analysis. The framework for feature extraction in this study is similar to the method used in [11]. In their work, 1074 frames of within-class variations data of HC and MI multi-lead ECG are used for evaluation. Each frame consists of four ECG beats. They have used DWT to decompose the ECG signal up to the 6th level of decomposition, whereas in this work, the VMD technique is implemented. In our study, subject-wise validation approach is performed [36]. 10,000 beats of MEKG, both from HC and MI, are utilised for analysis in this work. Comparative analysis of the results shows that our proposed method exhibited better performance than the DWT-based approach and other methods, as shown in Table 2.

4. Conclusions: In this study, a novel method to investigate the pathological characteristics of MI from MEKG is proposed. Normal and pathology MI MEKG signals are analysed using VMD based approach. Initially, the MEKG signal is preprocessed prior to further processing to remove low-frequency artefact and noise, among others. The noise-free signal is subjected to the VMD algorithm. The changes that are observed in the mode coefficients from the VMD caused the variations in the values of different features that can capture useful information from a given ECG signal. The multiscale mode energy is one such feature

acquired from the different decomposed mode that reflects the significant change of the pathological signal. Also, the interlead correlations of the MSMM affect the covariance structures, and the eigenvalues of the MSMM exhibit these changes. Therefore, the change in the ECG signal of a pathological signal can be represented by the computed eigenvalues and can be used as a feature. Hence, these extracted feature subsets can further be employed to train the classification models to discriminate between healthy control and MI. The proposed method achieved the highest classification performance from the SVM classifier with an RBF kernel and obtained 99.88% specificity, 99.90% sensitivity, and accuracy of 99.88%. The yielded results indicate that the proposed method is capable of successful detection of MI and achieved better results than existing methods.

5 References

- [1] Mendis S., Puska P., Norrving B.: 'Global atlas on cardiovascular disease prevention and control' (World Health Organization, Geneva, Switzerland, 2011)
- [2] Goldberger A.L.: 'Clinical electrocardiography: a simplified approach' (Elsevier Health Sciences, New York, NY, USA, 2012)
- [3] Thygesen K., Alpert J.S., Jaffe A.S., *ET AL.*: 'Third universal definition of myocardial infarction', *Circulation*, 2012, **126**, (16), pp. 2020–2035
- [4] Arif M., Malagore I.A., Afsar F.A.: 'Detection and localization of myocardial infarction using k-nearest neighbor classifier', *J. Med. Syst.*, 2012, **36**, pp. 279–289
- [5] Jaleel A., Tafreshi R., Tafreshi L.: 'An expert system for differential diagnosis of myocardial infarction', *J. Dyn. Syst. Meas. Control*, 2016, **138**, (11), p. 111012
- [6] Safdarian N., Dabanloo N.J., Attarodi G.: 'A new pattern recognition method for detection and localization of myocardial infarction using T wave integral and total integral as extracted features from one cycle of ECG signal', *Sci. Res. Publishing*, 2014, **7**, pp. 818–824
- [7] Remya R., Indiradevi K., Babu K.A.: 'Classification of myocardial infarction using multiresolution wavelet analysis of ECG', *Proc. Technol.*, 2016, **24**, pp. 949–956
- [8] Acharya U.R., Fujita H., Adam M., *ET AL.*: 'Automated characterization and classification of coronary artery disease and myocardial infarction by decomposition of ECG signals: a comparative study', *Inf. Sci.*, 2017, **377**, pp. 17–29
- [9] Jayachandran E.S., Joseph K.P., Acharya U.R.: 'Analysis of myocardial infarction using discrete wavelet transform', *J. Med. Syst.*, 2010, **34**, (6), pp. 985–992
- [10] Padhy S., Dandapat S.: 'Third-order tensor based analysis of multi-lead ECG for classification of myocardial infarction', *Biomed. Signal Process. Control*, 2017, **31**, pp. 71–78
- [11] Sharma L.N., Tripathy R.K., Dandapat S.: 'Multiscale energy and eigenspace approach to detection and localization of myocardial infarction', *IEEE Trans. Biomed. Eng.*, 2015, **62**, (7), pp. 1827–1837
- [12] Weng J.T., Lin J., Chen Y.C., *ET AL.*: 'Myocardial infarction classification by morphological feature extraction from big 12-lead ECG data'. Pacific-Asia Conf. on Knowledge Discovery and Data Mining, Cham, May 2014, pp. 689–699
- [13] Liu B., Liu J., Wang G., *ET AL.*: 'A novel electrocardiogram parameterization algorithm and its application in myocardial infarction detection', *Comput. Biol. Med.*, 2015, **61**, pp. 178–184
- [14] Tseng Y.-L., Lin K.-S., Jaw F.S.: 'Comparison of support vector machine and sparse representation using a modified rule-based method for automated myocardial ischemia detection', *Comput. Math. Methods Med.*, 2016, **2016**, pp. 1–8
- [15] Acharya U.R., Fujita H., Sudarshan V.K., *ET AL.*: 'Automated detection and localization of myocardial infarction using electrocardiogram: a comparative study of different leads', *Knowl.-Based Syst.*, 2016, **99**, pp. 146–156
- [16] Lahiri T., Kumar U., Mishra H., *ET AL.*: 'Analysis of ECG signal by chaos principle to help automatic diagnosis of myocardial infarction', *J. Sci. Ind. Res.*, 2009, **68**, (10), pp. 866–870
- [17] Maglaveras N., Stamkopoulos T., Pappas C., *ET AL.*: 'An adaptive backpropagation neural network for real-time ischemia episodes detection: development and performance analysis using the European ST-T database', *IEEE Trans. Biomed. Eng.*, 1998, **45**, (7), pp. 805–813
- [18] Hadjem M., Nat-Abdesselam F., Khokhar A.: 'ST-segment and T wave anomalies prediction in an ECG data using RUSBoost'. Proc. 2016 IEEE 18th Int. Conf. e-Health Netw., Appl. Services, Munich, Germany, September 2016, pp. 1–6
- [19] Sun L., Lu Y., Yang K., *ET AL.*: 'ECG analysis using multiple instance learning for myocardial infarction detection', *IEEE Trans. Biomed. Eng.*, 2012, **59**, (12), pp. 3348–3356
- [20] Achlerkar P.D., Samantaray S.R., Manikandan M.S.: 'Variational mode decomposition and decision tree based detection and classification of power quality disturbances in grid-connected distributed generation system', *IEEE Trans. Smart Grid*, 2016, **9**, (4), pp. 3122–3132
- [21] Das P., Manikandan M.S., Ramkumar B.: 'Detection of epileptic seizure event in EEG signals using variational mode decomposition and mode spectral entropy'. 2018 IEEE 13th Int. Conf. on Industrial and Information Systems (ICIIS), Rupnagar, India, 2018, pp. 42–47
- [22] Lal G.J., Gopalakrishnan E.A., Govind D.: 'Accurate estimation of glottal closure instants and glottal opening instants from electroglottographic signal using variational mode decomposition', *Circuits Syst. Signal Process.*, 2018, **37**, (2), pp. 810–830
- [23] Prabhakararao E., Manikandan M.S.: 'On the use of variational mode decomposition for removal of baseline wander in ECG signals'. 2016 Twenty-Second National Conf. on Communication (NCC), Guwahati, 2016, pp. 1–6
- [24] Lahmiri S.: 'Comparative study of ECG signal denoising by wavelet thresholding in empirical and variational mode decomposition domains', *Healthc. Technol. Lett.*, 2014, **1**, (3), pp. 104–109
- [25] Tripathy R.K., Sharma L.N., Dandapat S.: 'Detection of shockable ventricular arrhythmia using variational mode decomposition', *J. Med. Syst.*, 2016, **40**, (4), p. 79
- [26] Rangayyan R.M.: 'Biomedical signal analysis: a case-study approach' (ser. IEEE Press Series in Biomedical Engineering. IEEE Press, Piscataway, NJ, USA, 2002)
- [27] Manikandan S., Dandapat S.: 'Wavelet-based electrocardiogram signal compression methods and their performances: a prospective review', *Biomed. Signal Process Control*, 2014, **14**, pp. 73–107
- [28] Pan J., Tompkins W.J.: 'A real-time QRS detection algorithm', *IEEE Trans. Biomed. Eng.*, 1985, **32**, (3), pp. 230–236
- [29] Acharya U.R., Fujita H., Oh S.L., *ET AL.*: 'Application of deep convolutional neural network for automated detection of myocardial infarction using ECG signals', *Inf. Sci.*, 2017, **415–416**, pp. 190–198
- [30] Dragomiretskiy K., Zosso D.: 'Variational mode decomposition', *IEEE Trans. Signal Process.*, 2014, **62**, (3), pp. 531–544
- [31] Sharma L.N., Dandapat S., Mahanta A.: 'Multichannel ECG data compression based on multiscale principal component analysis', *IEEE Trans. Inf. Technol. Biomed.*, 2012, **16**, (4), pp. 730–736
- [32] Cortes C., Vapnik V.: 'Support-vector networks', *Mach. Learn.*, 1995, **20**, (3), pp. 273–297
- [33] Oeff M., Koch H., Bousseljot R., *ET AL.*: 'The ptb diagnostic ecg database', (National Metrology Institute of Germany, 2012). Available at <http://www.physionet.org/physiobank/database/ptbdb>
- [34] Cristianini N., Shawe-Taylor J.: 'an introduction to support vector machines and other kernel-based learning methods', (Cambridge Univ. Press, New York, NY, USA, 2000)
- [35] Liu W., Zhang M., Zhang Y., *ET AL.*: 'Real-time multilead convolutional neural network for myocardial infarction detection', *IEEE J. Biomed. Health Inf.*, 2017, **22**, (5), pp. 1434–1444
- [36] Ansari S., Farzaneh N., Duda M., *ET AL.*: 'A review of automated methods for detection of myocardial ischemia and infarction using electrocardiogram and electronic health records', *IEEE Rev. Biomed. Eng.*, 2017, **10**, pp. 264–298